Journal of Marine Science and Technology

Volume 23 | Issue 4 Article 16

THE NEW METHOD TO EVALUATE THE UPLIFT CAPACITY OF BELLED PILES IN SANDY SOIL

Jaw-Guei Lin
Department of Harbor and River Engineering, National Taiwan Ocean University, Keelung, Taiwan,
jglin@mail.ntou.edu.tw

Shih-Yu Hsu
Department of Harbor and River Engineering, National Taiwan Ocean University, Keelung, Taiwan

San-Shyan Lin
Department of Harbor and River Engineering, National Taiwan Ocean University, Keelung, Taiwan

Journal of Marine Science and Technology, Vol. 23, No. 4, pp. 523-533 (2015)
DOI: 10.6119/JMST-015-0511-2

THE NEW METHOD TO EVALUATE THE UPLIFT CAPACITY OF BELLED PILES IN SANDY SOIL

Jaw-Guei Lin, Shih-Yu Hsu, and San-Shyan Lin

Key words: belled pile, uplift capacity, foundation, sandy soil.

ABSTRACT

In conventional geotechnical engineering, the pull out of pile is always blamed only on the shear failure of the soil caused by the uplift force developed from the tip of the pile. For the belled pile, however, the enlarged foundation plays an important role to against the compression/uplift load, and the current theories for estimating the uplift capacities of the pile were found more than 50% relative error from measured. In this study, a new method for estimating the ultimate uplift capacity of the belled pile embedded in sandy soil was developed by taking into account the elastic/plastic behavior of the soil around the belled pile. It assumes that during the pull out process of the pile, the soil above the enlarged base is firstly subjected to an upward compression and causes a local soil consolidation which might affect the development of resultant failure surface of the soil around the pile. The starting location of failure surface is allowed to develop at a distance away from the pile surface. With 37 sets of experimental/field tests data, the development of the failure surface with curved slip-surface was suggested to start at the location of 0.67 of the radius of the enlarged base from central axis of the pile. The new method shows good approach with relative error lesser than 25% which is better than previous theories.

I. INTRODUCTION

Two types of pile foundations, point bearing pile and frictional pile, are usually designed to support the vertical loads from superstructures. The point bearing pile directly transmits the vertical load to the rock base beneath the subsoil, and the frictional pile overcomes the vertical load by the frictional resistance on the interface between the pile and the soil. To enhance the resistance, a frictional pile is better to employ an enlarged base to increase the contact surface, especially when the pile is embedded in sand. Such vertical pile with enlarged base is generally called belled pile, and has been proven to be an economical way to increase the bearing capacity and is widely applied in civil engineering. In normal situation, the pile is usually subjected to the vertical compression loads, however, it might also be subjected to the uplift force from bending moment or the lateral forces during earthquake, wind, tidal current, or waves actions or from the tension force of cables, such as transmission towers, mooring system for an offshore structures, jetties or pier structures, tall chimneys, and offshore wind towers, etc. which are constructed on the pile foundations.

Even though the major purpose of the enlarged base of pile foundation is to increase the bearing capacity, it can also increase the uplift resistant capacity when subjected to uplift loads. Verma et al. (2010) showed from their experiments that the belled pile offers higher uplift capacity than single pile. The increase uplift capacity by the enlarged foundation must be taken into account in engineering planning and design.

Many theories for estimating the uplift capacity of piles were developed based on different assumptions of the shapes of failure surface, but not specifically for belled pile. When pulling out a belled pile, the soil above the enlarged base will sustain an upward compression and cause a local consolidation. Compared to the single pile, such consolidation phenomenon of the belled pile should have some influence on the development of uplift resistance of the belled pile. This study is aimed at developing a suitable empirical method to properly estimate the uplift capacity of the belled pile. Thirty-seven sets of measured data from laboratory experiments/field tests were used to calibrate the starting location of resultant failure surface, an empirical equation was suggested, and the relative errors between estimated and measured uplift capacities were discussed.

In the following paragraphs of this section, we briefly review the previous theories about ultimate uplift capacities and the related empirical formulas. In section 2, the scope of this study will be stated. In section 3, the equations of failure surface and ultimate uplift capacity on the basis of Chattopadhyay and Pise (1986) with variable starting location of failure

Paper submitted 04/16/14; revised 03/13/15; accepted 05/11/15. *Author for correspondence: Jaw-Guei Lin (e-mail: jglin@mail.ntou.edu.tw).*
Department of Harbor and River Engineering, National Taiwan Ocean University, Keelung, Taiwan, R.O.C.

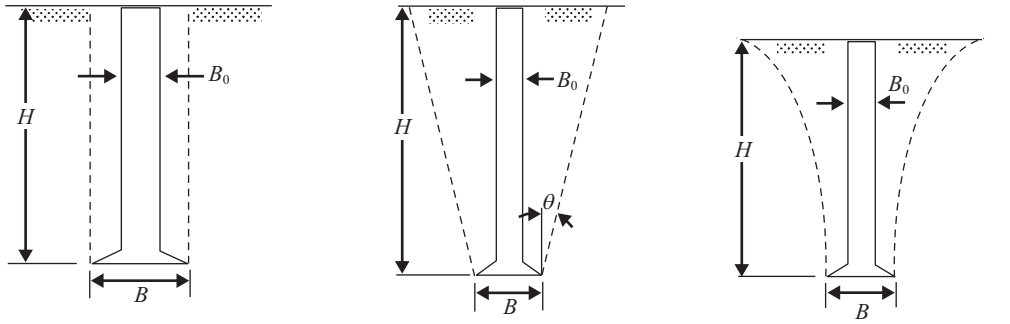

(a) Vertical slip surface model (b) Inverted truncated cone model (c) Curved slip-surface model

Fig. 1. The failure mechanisms of belled pile under uplift loads (Dickin, 1988).

surface will be derived. In section 4, some comparisons and discussions are made. At the end, there are conclusions and references.

1. Previous Studies about Ultimate Uplift Capacity

Researches on the uplift capacity of the pile foundation can be classified into three groups: horizontal anchor plate, single pile and belled pile. Shanker et al. (2007) had made a brief review, and only those related to belled piles are discussed here. Dickin (1988) classified the failure mechanisms for belled piles subjected to uplift load, as shown in Fig. 1, into three categories: (a) vertical slip surface model; (b) inverted truncated cone model, and (c) curved slip-surface model. In each figure, B_0 is the diameter of the vertical pile, B is the diameter of the enlarged base, H is the embedded length of the pile, and θ is the inclination angle of the failure surface.

The vertical slip surface model, as shown in Fig. 1(a), was first proposed by Majer in 1955 who assumed a vertical slip surface above the anchor, where the uplift capacity is equal to the weights of the pile and the soil above the belled base plus the shearing resistance along the perimeter of the vertical slip surface with the same size of the anchor. The inverted truncated cone model, as shown in Fig. 1(b), assumed the total uplift force is equal to the sum of the weight of the pile and the soil in an inverted cone above the belled base surrounding the pile plus the shearing resistance along the perimeter of the failure surface. Downs and Chieurzzi (1966) and Murry and Geddes (1987) suggested that the inclination angle of the failure surface θ was equal to the friction angle of the soil, ϕ. Whereas, Clemence and Veesaert (1977) proposed that the angle θ was equal to $\phi/2$. Sutherland et al. (1983) pointed out, from a series of laboratory experiments on anchors, that the angle of inclination of the inverted truncated cone slip surface to the vertical axis was a function of soil friction angle and relative density, that is, $\theta = F(\phi, \gamma)$. Vermeer and Sutjiadi (1985) proposed that θ was equal to the dilatancy angle ψ of the soil. For curved slip-surface model, as shown in Fig. 1(c), Balla (1961) firstly noted that the slip surface above small model anchors was a tangential curve, whereas Meyerhof and Adams (1968) observed a pyramidal shaped slip surface above the anchor in laboratory model tests. Subsequently, Vesic (1971) employed a shallow cavity expansion model to determine the uplift capacity. Based on a series of laboratory experiments and field tests on anchors, Andreadis and Harvey (1981) developed design charts to determine the uplift resistance of anchors, Ovesen (1981) obtained a relationship for the uplift capacity of the anchor plates from his centrifugal model tests. Rowe and Davis (1982) employed a finite-element analysis incorporating an elastic-plastic soil model to determine the uplift capacity of horizontal strip anchors. The capacity of the belled piles can be derived from this theory by use of a suitable shape factor, e.g., Dickin (1988) and Frydman and Shaham (1989).

Ghaly et al. (1991) collected the results from Meyerhof and Adams (1968), Sutherland et al. (1983) and Clemence and Veesaert (1977). He classified the observed failure categories of screw anchor pile into three types as shown in Fig. 2 where the dotted line is the observed failure surface, and the solid line is the suggested theoretical failure surface. For shallow foundation, the sectional failure surface is a curve type; for deep foundation, the failure surface becomes a bulb type; and for the intermediate depth foundation, the failure surface becomes a vane type. They suggested the inverted cone slip surface for the analysis. In deep foundation cases, however, the shear resistance of soil was neglected.

Dickin et al. (1983 and 1988) investigated the failure surface of anchor plate via centrifuge tests and found the deep anchored plate has bulb type failure surface, and the medium anchored plate has curve-slip surface.

2. Existing Formula of Ultimate Uplift Capacity

To facilitate the determination of the uplift capacity for easy engineering applications, simple expressions and accompanying design charts are often provided. The net ultimate uplift resistance, $P_{u,Net}$, is usually expressed in terms of a dimensionless breakout factor $N_u = P_{u,Net}/(\gamma_S A_b H)$, where γ_S is the unit weight of soil, A_b is the area of the enlarged base and H is the embedded length of belled pile. Dickin and Leung (1990) summarized the formulas of the breakout factor proposed by a number of researchers. Only the formulas related to the pile were revised here.

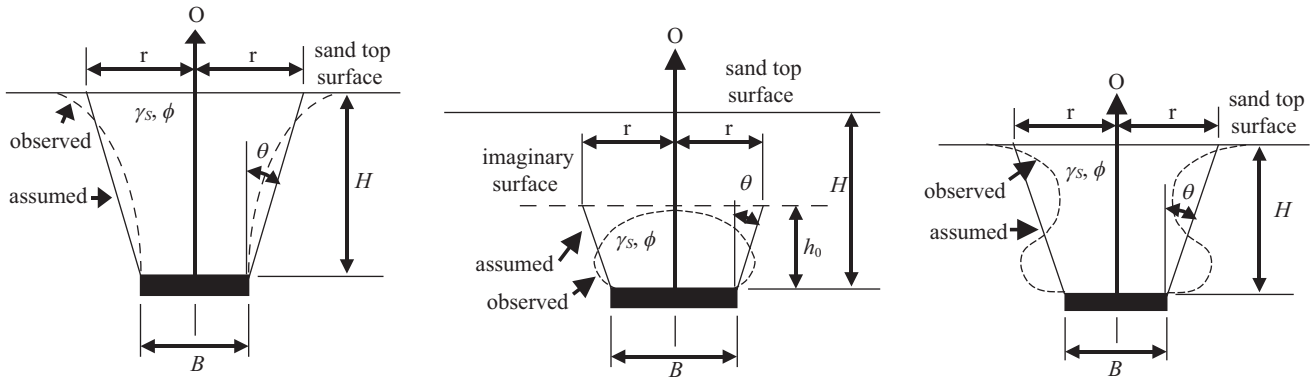

(a) Shallow foundation (b) Deep foundation (c) intermediate depth foundation

Fig. 2. The failure modes of screw anchor piles (Ghaly et al., 1991).

(1) Balla (1961) assumed the tangential-curve slip surface, and derived the following equation

$$\left(N_u\right)_B = (F_1 + F_3)\left(4/\pi\right)\left(H/B\right)^2 \tag{1}$$

where F_1 and F_3 are functions of peak friction angle ϕ and γ_S which are obtained from the chart provided by Balla (1961). F_1 and F_3 have the following relation.

$$F_1 + F_3 = -0.0171\left(H/B\right)^3 + 0.3057\left(H/B\right)^2 - 1.7937\left(H/B\right) + 4.0389$$

(2) Downs and Chieurzzi (1966) assumed the inverted truncated cone slip surface and the cone angle with vertical axis is equal to ϕ, and derived the following equation

$$\left(N_u\right)_{D\&C} = 1 + 2\left(L/B\right)\tan\phi + \left(4/3\right)\left(H/B\right)^2 \tan^2\phi + \left(B_0/B\right)^2 \tag{2}$$

(3) Meyerhof and Adams (1968) assumed the pyramidal-shaped slip surface, Das and Yang (1987) modified their theory and derived the following equation

$$\left(N_u\right)_{M\&A} = 2\left(H/B\right)\tan\phi * K_u * \left[m\left(H/B\right) + 1\right] + 1 \tag{3}$$

where $K_u = 0.9$ for $30° < \phi < 45°$, and m is the shape factor which is function of ϕ.

(4) Ovesen (1981) derived an equation from the centrifugal model tests on horizontal anchor plates.

$$\left(N_u\right)_O = 1 + \left(4.32 * \tan\phi - 1.58\right)\left(H/B_e\right)^{1.5} \tag{4}$$

where $B_e = \sqrt{\pi B^2/4}$.

(5) Surtherland et al. (1982) assumed the inverted truncated cone slip surface and the cone angle with vertical axis is function of ϕ, and derived the following equation

$$\left(N_u\right)_S = \frac{8}{3}\left(H/B\right)^2 \tan^2\alpha + 4\left(H/B\right)\tan\alpha + 1 \tag{5}$$

where $\alpha = 0.25\left[I_D\left(1 + \cos^2\phi\right) + 1 + \sin^2\phi\right]\phi$ and I_D is the soil density index with suggested value of 0.6.

(6) Murray and Geddes (1987) assumed the inverted truncated cone slip surface and the cone angle with vertical axis is equal to ϕ, and derived the following equation

$$\left(N_u\right)_{M\&G} = 1 + \left(H/B_e\right)\tan\phi\left[2 + \left(\pi/3\right)\left(H/B_e\right)\tan\phi\right] \tag{6}$$

(7) Chattopadhyay and Pise (1986) assumed the curved slip-surface as function of ϕ and λ, and derived the following equation

$$\left(P_{u,Net}\right)_{C\&P} = P_u - W_{pile} = A\gamma_S \pi B_m H^2 - W_{pile} \tag{7}$$

where

$$A = \int_0^H 2\left(x_m / B_m\right)\left(1 - z/H\right)\left[\cot\theta + \left(\cos\theta + K\sin\theta\right)\tan\phi\right] d\left(z/H\right)$$

All these theories assumed that the failure surface is developed from the surface of the vertical pile.

Table 1 shows some measured data from field tests and laboratory experiments about the uplift capacity of belled pile. Totally there are 37 data sets including 27 sets of field tests with 2 sets from Dickin (1990), 5 sets from Balla (1961), 4 sets from Kulhawy (1985), and 16 sets from Tucker (1987) and the other 10 sets of laboratory experiments from Balla (1961). In

Table 1. Measured uplift capacities and related characteristics of the belled piles (Lin, 1998).

No.	H (m)	B_0 (m)	B (m)	γ_S (kN/m^3)	ϕ (deg)	λ	$(P_u)_{test}$ (kN)	Remark
1	4.00	0.5000	1.00	30.00	32	4.00	644.000	Dickin (1990) Field tests
2	6.00	0.5000	1.00	30.00	32	6.00	1196.000	
3	1.50	0.6330	1.90	19.13	36	0.79	208.950	Balla (1961) Field tests
4	1.45	0.6330	1.90	19.13	36	0.76	209.930	
5	2.50	0.4333	1.30	16.28	30	1.92	204.050	
6	2.70	0.3667	1.10	13.05	30	2.45	243.290	
7	2.50	0.4667	1.40	15.70	30	1.79	230.830	
8	1.68	0.5100	1.22	18.86	38	1.38	174.440	Tucker (1987) Field tests
9	1.68	0.5100	1.22	18.86	40	3.29	115.700	
10	3.08	0.4700	0.61	19.80	31	5.05	156.640	
11	2.77	0.4600	0.75	19.80	31	3.69	180.225	
12	2.83	0.4600	1.01	19.80	31	2.80	235.850	
13	3.17	0.4800	1.03	19.80	31	3.08	226.950	
14	2.03	1.0900	1.30	17.13	40	1.56	288.810	
15	1.73	0.9100	1.22	17.13	40	1.42	231.400	
16	2.18	0.9100	1.27	17.13	40	1.72	220.280	
17	2.11	0.9100	1.32	19.49	42	1.60	399.170	
18	2.53	0.8400	1.37	17.29	40	1.85	469.920	
19	2.29	0.8400	1.52	19.33	42	1.51	521.990	
20	3.20	0.4600	0.91	16.97	36	3.52	445.000	
21	3.20	0.4600	0.91	17.76	36	3.52	339.090	
22	2.35	0.6100	1.13	17.92	33	2.08	273.230	
23	4.27	0.6100	0.91	18.07	31	4.69	299.930	
24	2.74	0.6100	0.91	18.86	36	3.01	243.290	Kulhawy (1985) Field tests
25	3.35	0.6100	0.91	18.86	36	3.68	534.650	
26	1.22	0.6100	0.91	18.86	36	1.34	127.530	
27	1.98	0.6100	0.91	17.29	30	2.18	201.110	
28	0.20	0.0100	0.03	19.00	37	6.67	0.03924	Balla (1961) Laboratory experiments
29	0.20	0.0200	0.06	19.00	37	3.33	0.14715	
30	0.20	0.0300	0.09	19.00	37	2.22	0.19130	
31	0.20	0.0400	0.12	19.00	37	1.67	0.22073	
32	0.05	0.0300	0.09	19.00	37	0.56	0.01668	
33	0.10	0.0300	0.09	19.00	37	1.11	0.05003	
34	0.15	0.0300	0.09	19.00	37	1.67	0.10301	
35	0.20	0.0300	0.09	19.00	37	2.22	0.19130	
36	0.25	0.0300	0.09	19.00	37	2.78	0.30901	
37	0.30	0.0300	0.09	19.00	37	3.33	0.39731	

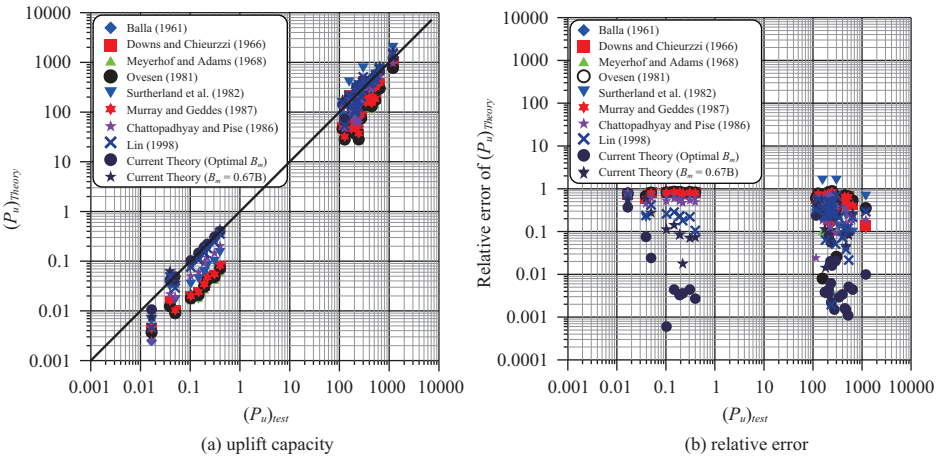

Fig. 3. Comparisons of $(P_u)_{Theory}$ and $(P_u)_{Test}$ (P_u unit: kN).

Table 2. Comparisons of $(P_u)_{Theory}$ and optimal B_m values.

No.	Measured	Estimated								Current Theory with optimal B_m			Current Theory with $B_m = 0.67B$		
	$(P_u)_{Test}$ (kN)	$(P_u)_{B}$ (kN)	$(P_u)_{D\&C}$ (kN)	$(P_u)_{M\&A}$ (kN)	$(P_u)_{O}$ (kN)	$(P_u)_{S}$ (kN)	$(P_u)_{M\&G}$ (kN)	$(P_u)_{C\&P}$ (kN)	$(P_u)_{Lin}$ (kN)	B_m/B	$(P_u)_{OPT}$ (kN)	$\varepsilon_r(P_u)$	B_m/B	$(P_u)_{0.67B}$ (kN)	$\varepsilon_r(P_u)$
1	644.0000	343.6680	372.1304	301.1426	299.5219	705.9727	382.1303	528.4041	783.0840	0.5600	646.8061	0.0044	0.6700	813.5789	0.2633
2	1196.0000	1005.9930	1025.5755	817.7799	772.9917	1995.1913	1052.1616	968.1129	1540.4785	0.5600	1207.8984	0.0099	0.6700	1589.4436	0.3290
3	208.9500	48.4295	58.6753	50.4272	50.2700	90.7636	59.4646	68.1698	110.1646	1.0000	208.0298	0.0044	0.6700	152.0913	0.2721
4	209.9300	45.1938	56.4260	48.5899	48.1804	86.6329	57.0991	61.8813	100.7943	1.0000	193.0970	0.0802	0.6700	140.9986	0.3284
5	204.0500	71.2739	47.1152	41.1336	37.1415	82.6566	48.7628	82.0502	158.0009	0.6700	203.3077	0.0036	0.6700	203.3077	0.0036
6	243.2900	50.7973	35.8000	31.0387	28.1815	64.9932	37.1660	60.5617	123.3112	1.0000	239.4062	0.0160	0.6700	159.0746	0.3462
7	230.8300	75.7622	49.9952	43.7359	39.3691	86.6783	51.6679	86.2568	163.7516	0.7300	229.3921	0.0062	0.6700	211.0453	0.0857
8	174.4400	47.0398	45.0961	35.8368	41.4588	77.6953	46.0359	101.8766	136.0528	0.8000	175.1033	0.0038	0.6700	154.7401	0.1129
9	115.7000	47.0398	48.7639	37.8034	45.9385	85.0311	49.8930	118.4936	153.6225	0.5000	143.2284	0.2379	0.6700	172.6003	0.4918
10	156.6400	198.8009	212.4760	171.7353	157.8933	401.6372	214.4513	184.9019	210.6645	0.7705	195.5610	0.2485	0.7705	195.5610	0.2485
11	180.2250	118.9670	117.3568	96.2875	91.3896	218.1033	119.1921	149.4467	191.5889	0.6800	180.9317	0.0039	0.6700	177.6582	0.0142
12	235.8500	112.2071	90.4357	75.8048	72.6413	165.5548	92.8698	154.0251	236.3111	0.6100	235.3199	0.0022	0.6700	261.4201	0.1084
13	226.9500	142.6443	122.4028	102.2365	97.8335	226.2766	125.7310	198.0944	303.0642	0.5000	231.5362	0.0202	0.6700	330.7222	0.4572
14	288.8100	195.3011	216.8494	152.4054	189.6352	354.7983	204.8279	261.9585	274.1584	0.8385	294.7512	0.0206	0.8385	294.7512	0.0206
15	231.4000	105.1768	116.0648	83.7976	102.4148	190.0242	111.0653	160.0874	173.1608	1.0000	218.4801	0.0558	0.7459	180.0166	0.2221
16	220.2800	167.6383	180.3353	129.7121	164.0177	309.6231	176.7186	285.3989	310.9543	0.7165	310.5846	0.4100	0.7165	310.5846	0.4100
17	399.1700	172.0955	199.9071	141.5930	185.2776	345.0178	196.9372	339.1365	370.6069	0.7900	397.8245	0.0034	0.6894	367.2296	0.0800
18	469.9200	188.8601	200.9816	146.4047	187.2229	356.0977	201.5557	397.4349	452.1179	0.7200	469.2001	0.0015	0.6700	448.2253	0.0462
19	521.9900	161.1359	182.9968	133.7211	173.0315	320.4481	184.2098	395.8431	458.7699	0.7900	522.5419	0.0011	0.6700	474.0050	0.0919
20	445.0000	119.0783	148.3938	110.8765	131.1715	281.9069	152.3376	293.2230	392.2751	0.7500	445.6912	0.0016	0.6700	401.9375	0.0968
21	339.0900	124.6217	155.3020	116.0381	137.2779	295.0304	159.4293	306.8733	410.5365	0.5400	340.0623	0.0029	0.6700	420.6488	0.2405
22	273.2300	112.2186	88.6420	71.7535	74.5782	155.4448	89.4057	160.4324	206.2368	0.8900	273.6332	0.0015	0.6700	213.3718	0.2191
23	299.9300	378.1868	406.8529	331.4624	307.6570	770.0306	413.1687	411.9156	509.1557	0.6703	434.9184	0.4501	0.6703	434.9184	0.4501
24	243.2900	169.5063	190.1058	141.5415	167.6097	350.6386	191.8556	307.4457	352.3292	0.6703	323.0212	0.3277	0.6703	323.0212	0.3277
25	534.6500	237.0679	309.3821	227.5826	268.8383	582.8075	313.8778	472.0330	546.1599	0.7300	531.9146	0.0051	0.6703	490.9707	0.0817
26	127.5300	35.2889	33.5586	25.7385	28.0714	53.4512	32.1245	46.9885	53.4989	1.0000	73.1322	0.4265	0.6703	54.1861	0.5751
27	201.1100	88.5459	63.3197	52.0177	47.1486	106.8196	61.9961	84.1362	99.9655	1.0000	140.2430	0.3027	0.6703	94.5749	0.5297
28	0.0392	0.0118	0.0156	0.0108	0.0124	0.0308	0.0160	0.0218	0.0485	0.5000	0.0422	0.0751	0.6700	0.0622	0.5846
29	0.1472	0.0185	0.0232	0.0172	0.0210	0.0444	0.0240	0.0602	0.1052	0.8000	0.1465	0.0044	0.6700	0.1263	0.1414
30	0.1913	0.0348	0.0330	0.0256	0.0308	0.0611	0.0343	0.0925	0.1474	0.7500	0.1907	0.0033	0.6700	0.1752	0.0844
31	0.2207	0.0512	0.0456	0.0364	0.0423	0.0814	0.0473	0.1178	0.1810	0.6900	0.2215	0.0036	0.6700	0.2168	0.0176
32	0.0167	0.0025	0.0044	0.0038	0.0037	0.0063	0.0044	0.0025	0.0046	1.0000	0.0106	0.3673	0.6700	0.0076	0.5419
33	0.0500	0.0101	0.0100	0.0083	0.0090	0.0167	0.0103	0.0191	0.0291	1.0000	0.0488	0.0241	0.6700	0.0363	0.2736
34	0.1030	0.0216	0.0192	0.0154	0.0179	0.0343	0.0199	0.0497	0.0763	0.7900	0.1031	0.0006	0.6700	0.0915	0.1119
35	0.1913	0.0348	0.0330	0.0256	0.0308	0.0611	0.0343	0.0925	0.1474	0.7500	0.1907	0.0033	0.6700	0.1752	0.0844
36	0.3090	0.0484	0.0524	0.0396	0.0484	0.0990	0.0544	0.1446	0.2410	0.7300	0.3076	0.0044	0.6700	0.2873	0.0702
37	0.3973	0.0626	0.0781	0.0580	0.0710	0.1497	0.0810	0.2032	0.3550	0.6200	0.3984	0.0027	0.6700	0.4264	0.0733

the table, the embedded length H, the diameter of pile B_0, the diameter of enlarged base B, the soil density γ_S, the friction angle of soil ϕ, the slenderness of pile $\lambda(= H/B_0)$, and the net uplift capacity $(P_u)_{Test}$ are recorded. The comparisons between the estimated ultimate uplift capacities from all existing theories and the measured uplift capacities of 37 data sets and their relative errors can be seen in Fig. 3 and from column 3 to column 9 in Table 2. Fig. 3(a) is the relation of estimated value P_u *vs*. measured value $(P_u)_{Test}$. The data appears in two groups, one from laboratory experiments, and the other one from field tests. The figure shows that all estimated value from previous theories is under-estimated which implies that some influence factors are missing. Table 3 shows the relative errors between estimated uplift capacity P_u and measured data $(P_u)_{Test}$ for all theories. The relative error of P_u, $\varepsilon_r(P_u)$ is defined as

$$\varepsilon_r = \left| \frac{P_u - (P_u)_{Test}}{(P_u)_{Test}} \right| \tag{8}$$

As can be seen in Table 3, the relative errors for the first six theories are all greater than 50% because they are concerned about the pile without enlarged base. Chattopadhyay and Pise (1986) assumed the curved resultant failure surface developed from the tip of the vertical pile, the relative errors are still greater than 39%. Nevertheless, the assumption of curve resultant failure surface is still better than other theories.

Under such circumstance, Lin (1998) applied the theory of Chattopadhyay and Pise (1986) for vertical pile foundation on the belled pile foundation by assuming that the failure surface develops from the gravity center of the enlarged base surface, $B_0/2 + (B - B_0)/6$, instead of from the vertical pile surface,

Table 3. Relative errors of estimated $(P_u)_{Theory}$ from different theories (for 37 data sets).

Relative Error	$(P_u)_B$ (1961)	$(P_u)_{D\&C}$ (1966)	$(P_u)_{M\&A}$ (1968)	$(P_u)_O$ (1981)	$(P_u)_S$ (1982)	$(P_u)_{M\&G}$ (1987)	$(P_u)_{C\&P}$ (1986)	$(P_u)_{Lin}$ (1998)	$(P_u)_{OPT}$ (optimal B_m)	$(P_u)_{0.67B}$ ($B_m = 0.67B$)
Averaged	0.6094	0.6041	0.6718	0.6368	0.5022	0.6018	0.3943	0.2827	0.0849	0.2475
Standard deviation	0.2036	0.2080	0.2024	0.2251	0.3350	0.2049	0.2170	0.1820	0.1449	0.1780
Confidence interval	0.0656	0.0670	0.0652	0.0725	0.1080	0.0660	0.0699	0.0586	0.0467	0.0648

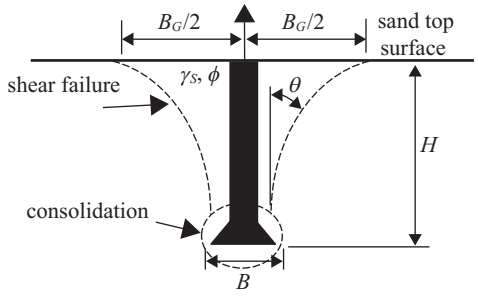

Fig. 4. Proposed failure category of the belled pile.

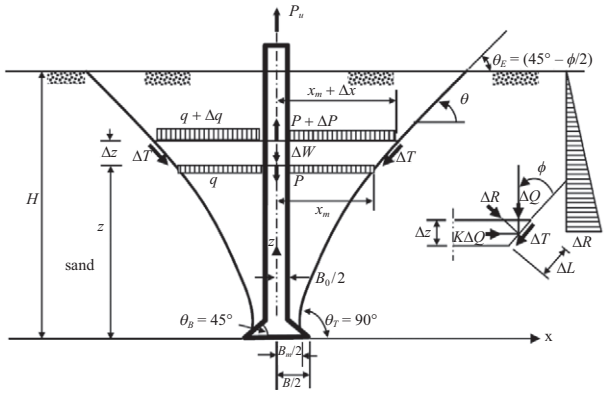

Fig. 5. Definition sketch and free body diagram of the resultant shear failure surface of the belled pile.

$B_0/2$. The estimated $(P_u)_{Lin}$ is shown in column 10 in Table 2, and the relative error $\varepsilon_r(P_u)$ is shown in column 9 in Table 3. The results are also shown in Fig. 3 with symbol of ✖, the estimated value is slightly smaller than the test data. The averaged relative error of Lin's theory is around 28% (see Table 3) which shows great improvements from the previous theories. The assumption of the starting location of resultant failure surface developed from the gravity center of the enlarged base, however, might be affected by the shape of the base where it is not definitely triangle.

II. SCOPE OF STUDY

According to the contributions from the previous studies about the pullout resistance and the resultant failure surface of the piles, the process of the pile-soil behavior when subjected to an uplift force to failure can be concluded. When pulling out a belled pile, the increased uplift force, after the force overcomes the pile weight, will act upwardly on the soil above the enlarged base. With the resistance induced from the soil weight, the soil consolidation occurs. According to the Boussinesq's theory or Mindlin's theory of soil stress distributions, the density of the consolidated soil above the base should be varied in distance. It will be denser near to the upper surface of the base, and decade to the normal soil density at some distance, instead of uniformly distributed. Such soil consolidation phenomenon should affect the development of resultant failure surface and the uplift capacity of the belled pile. For example, the dense soil near by the enlarged base might act like part of the base.

A new theory on estimating the uplift capacity of the belled pile adjusted from Lin's theory (1998) is proposed in this paper, the failure mechanism of the belled pile is divided into two parts as shown in Fig. 4. Basically, the belled pile is assumed to be the combination of a vertical pile and an anchor plate. Similar to the uplift behavior of the screw anchor pile, the resultant failure surface is assumed to be a vane type as shown in Fig. 2(c) which is a combination of a bulb caused by the soil consolidation above the enlarged base and a curved slip-surface caused by the shear failure of soil. For shallow foundation, due to the soil above the base is thinner, there is not enough resistance to against the uplift force and therefore the vane type failure is unapparent, and the shear failure of soil takes the role as shown in Fig. 2(a). For deep foundation, due to the soil above the base is thick, the soil can be fully consolidated, and the upward deformation of the soil (bulb type) reaches the criteria of pullout failure before the development of the shear failure of the soil as shown in Fig. 2(b).

The total uplift capacity of the belled pile is still assumed to be the sum of the pile weight, the soil weight bounded by the failure surface and the shear resistance along the failure surface, but allows the starting location of the failure surface can start at some suitable location on the enlarged base. The theory of Chattopadhyay and Pise (1986) is still employed in this study but with different location of the shear failure surface.

III. ESTIMATION OF ULTIMATE UPLIFT CAPACITY

In this section, the estimation of shear resistance of the soil due to the uplift force is discussed. Fig. 5 shows a free body diagram of belled pile and related failure surface. A belled circular pile with diameter of vertical pile B_0 and an enlarged

base of truncated cone with diameter of B embedded at depth H in sandy soil with effective unit weight γ_S and angle of shearing resistance ϕ. The Cartesian coordinates system is used in the derivation where the origin is set at the bottom of the enlarged base and at the central axis of the pile with x-axis horizontally positive to the right and z-axis vertically positive upwardly. When the pile is subjected to a lifting force, the surrounding soil will induce an uplift resistance and the pile will be pulled out after the uplift force overcomes the resistance.

Similar to Chattopadhyay and Pise (1986), the resultant failure surface was assumed to be an axial symmetrical solid body of soil revolved along with the central axis of the pile (see Fig. 5). Considering the interlock effect of the soil particles above the enlarged base might cause the resulting failure surface developed away from the pile surface, however, the starting location of the resulting surface is allowed detached from pile surface ($B_0/2$) and lies within $B_0/2$ and $B/2$ which is different from Lin (1998) where the surface is start from the gravity center of the enlarged base, and from Chattopadhyay and Pise (1986) where the surface is start from the surface of vertical pile.

1. Derivation of Resultant Failure Surface

Referring to Chattopadhyay and Pise (1986) and considering the characteristics of the belled pile, the assumptions about the resultant failure surface of the belled pile were made as follows.

(1) The shape and extent of failure surface are assumed affected by the slenderness ratio λ, the angle of shearing resistance ϕ and the pile-soil friction angle δ. For a particular λ, the maximum lateral horizontal extent of the failure surface from the central axis of pile occurs for $\delta = \phi$, and is gradually decreased with the decrease of δ. The lateral horizontal extent of the failure surface will increase with a rate as λ increases, and attains to a limit value at ground surface when λ approaches to infinity. When $\delta = 0$, however, the failure surface is parallel to the interfacial plane of the pile and the soil, instead of coincide with that interfacial plane. That is, the intersect angle of failure surface to horizontal ground surface is 90°.

(2) For piles with $\delta > 0$, the intersect angle of the failure surface to horizontal ground surface is assumed approaches to $(45° - \phi/2)$.

(3) For piles with $\delta \geq 0$ subjected to ultimate uplift force P_u, the failure surface starts tangentially to the pile surface at the some distance from the tip of the pile and moves through the surrounding soil.

The assumptions of (2) and (3) are different from the assumptions of Chattopadhyay and Pise (1986) due to the existence of the enlarged base. With the above assumptions and further assuming the resultant failure surface starts from ($B_m/2$, 0), where B_m lies within B_0 and B, the slope of the failure surface at any height z above the tip of the pile can be expressed as

$$\frac{dz}{dx} = \tan(45° - \frac{\phi}{2}) \frac{H}{z} \cdot e^{\beta\left(1-\frac{z}{H}\right)} \tag{9}$$

where, according to the assumptions of Chattopadhyay and Pise (1986), the maximum value of ϕ is set at 50° for practical purpose, that is

$$\beta = \frac{\lambda_m (50° - \phi)}{2\delta}, \text{ and } \lambda_m = \frac{H}{B_m} \tag{10}$$

where, λ_m is the slenderness of the soil column bounded by the failure surface.

Eq. (9) should satisfy the boundary conditions, that is, the inclination angle of the surface at the tip of the pile ($z = 0$) is $\theta_T = 90°$, and at the ground surface ($z = H$) is $\theta_E = (45° - \phi/2)$.

Integrating Eq. (9) with respect to z, we get

$$x_m = x + \frac{B_m}{2} = \frac{He^{-\beta\left(1-\frac{z}{L}\right)}}{\beta \tan(45° - \phi/2)} \left(\frac{z}{H} - \frac{1}{\beta}\right) + \frac{B_m}{2} + C \tag{11}$$

Since the failure surface is assumed to develop from ($B_m/2$, 0), C can be found as

$$C = \frac{He^{-\beta}}{\beta^2 \tan(45° - \phi/2)} \tag{12}$$

Therefore, we get the general solution

$$\frac{x_m}{B_m} = \frac{1}{2} + \frac{\lambda_m e^{-\beta}}{\beta^2 \tan(45° - \phi/2)} + \frac{\lambda_m e^{-\beta}}{\beta \tan(45° - \phi/2)} e^{\beta\left(\frac{z}{L}\right)} \left(\frac{z}{H} - \frac{1}{\beta}\right) \tag{13}$$

At ground surface ($z = H$), the extent distance (x_G) of the failure surface is

$$\frac{x_G}{B_m} = \frac{1}{2} + \frac{\lambda_m e^{-\beta}}{\beta^2 \tan(45° - \phi/2)} + \frac{\lambda_m}{\beta \tan(45° - \phi/2)} \left(1 - \frac{1}{\beta}\right) \tag{14}$$

2. Derivation of Uplift Capacity P_u

Assuming that at the moment of the pile to be pulled out, a resultant failure surface will be developed and the uplift force will reach to maximum. At that critical moment, the induced shear strength of the soil along the failure surface and the weights of the body of soil and pile will balance with the total applied uplift forces $P_{u,Gross}$. Considering a circular disc wedge of thickness Δz at height z above the pile tip inside the 3-D axial symmetrical failure surface, the inclination angle of the failure surface to the horizontal plane is θ.

For evaluating the shear resistance ΔT along the failure surface of the wedge with length ΔH, it is assumed that $\Delta T = \Delta R \tan\phi$, where $\Delta R = \Delta Q(\cos\theta + K \sin\theta)$ is the normal force

acting on the failure surface; $\Delta Q = \gamma_S(H - z - \Delta z/2)\Delta H$; $K = K_o(\tan\delta/\tan\phi)$ is the coefficient of lateral earth pressure generated within the wedge; $K_o = (1 - \sin\phi)$. When $\delta = \phi$, $K = K_o$. Thus

$$\Delta R = \gamma_S\left(H - z - \frac{\Delta z}{2}\right)\frac{\Delta z}{\sin\theta}\left(\cos\theta + K\sin\theta\right) \quad (15a)$$

and

$$\Delta T = \gamma_S\left(H - z - \frac{\Delta z}{2}\right)\frac{\Delta z}{\sin\theta}\left(\cos\theta + K\sin\theta\right)\tan\phi \quad (15b)$$

where $\sin\theta \approx \Delta z/\Delta H$.

Considering the balance of vertical forces of the wedge, and deducting the weight of the pile of length Δz, we have

$$\Delta P + q\pi\left(x_m^2 - \left(\frac{B_0}{2}\right)^2\right) - \left(q + \Delta q\right)\pi\left(\left(x_m + \Delta x\right)^2 - \left(\frac{B_0}{2}\right)^2\right)$$

$$-\Delta W - 2\pi\left(x_m + \frac{\Delta x}{2}\right)\Delta T\sin\theta = 0 \quad (16)$$

Define the volume of the circular disc wedge to be

$$\Delta W = \gamma_S\frac{\pi\Delta z}{3}\left[\left(x_m + \Delta x\right)^2 + x_m^2 + x_m\left(x_m + \Delta x\right)\right]$$

$$= \gamma_S\pi\Delta z\left[x_m^2 + x_m\Delta x + \frac{\Delta x^2}{3}\right] \quad (17)$$

and substituting the relation from Eq. (15b) and the relations of $q = \gamma_S(H - z)$ and $\Delta q = -\gamma_S\Delta z$ into Eq. (16), and neglecting the higher order terms like Δx^2, Δz^2, $\Delta x\Delta z$, $\Delta x\Delta q$, $\Delta x^2 q$ and $\Delta x^2\Delta z$, we get a simplified derived equation of uplift force of circular disc wedge

$$dP = 2\gamma_S\pi x_m\left(H - z\right)\left[\cot\theta + \left(\cos\theta + K\sin\theta\right)\tan\phi\right]dz \quad (18)$$

where $\cos\theta = dx/dz$.

Therefore, the net uplift capacity $P_{u,Net}$ of the belled pile for shear failure is given by

$$P_{u,Net} = \int_0^H dP = G_{us}\gamma_S\pi B_m H^2 \quad (19)$$

where, G_{us} is uplift capacity factor for shear failure,

$$G_{us} = \int_0^H 2\frac{x_m}{B_m}\left(1 - \frac{z}{H}\right)\left[\cot\theta + \left(\cos\theta + K\sin\theta\right)\tan\phi\right]d\left(\frac{z}{H}\right) \quad (20)$$

and the total ultimate uplift capacity $P_{u,Gross}$ can be given by

$$P_{u,Gross} = P_{u,Net} + W_{pile} = G_{us}\gamma_S\pi B_m H^2 + W_{pile} \quad (21)$$

where, W_{pile} is the weight of the belled pile,

$$W_{pile} = \gamma_{pile}\pi\left[\frac{\left(2H - B + B_0\right)B_0^2}{8} + \frac{\left(B - B_0\right)\left(B^2 + B_0^2 + BB_0\right)}{24}\right] \quad (22)$$

and γ_{pile} is the unit weight of the pile.

IV. COMPARISONS AND DISCUSSIONS

In order to find the optimal B_m value, a series of trial and error tests was carried out on 37 data sets by altering the B_m value and comparing their relative errors of estimated uplift capacity, $\varepsilon_r(P_u)$. During the tests, the B_m/B value is set as $1 \geq B_m/B \geq B_0/B$ which means the starting location (B_m) should not be outside the enlarged base or be inside the vertical pile. Columns 11 to 13 in Table 2 show the results, including the optimal B_m/B, uplift capacity $P_{u,Net}$, and relative error, $\varepsilon_r(P_u)$.

The averaged optimal B_m/B is 0.7599 ± 0.0511, and the averaged $\varepsilon_r(P_u)$ is 0.0849 ± 0.0467 (column 10 in Table 3). The results are also shown in Fig. 3 with symbol of ●, the estimations are found to be the best approaches in all theories. Although the variable B_m/B shows the best fit to the test data, the ratio is not identical and is difficult for practical use. Fig. 6 shows some observations about the relation of pile scale (H/B), soil frictional angle (ϕ) and uplift capacity. The data was classified into two groups according to the frictional angle ϕ, that is, $30° \leq \phi \leq 35°$ (▲) for loose sand and $35° < \phi \leq 42°$ (●) for dense sand. Fig. 6(a) shows relations of $\varepsilon_r(P_u)$ *vs.* ϕ, and Fig. 6(b) shows relations of the optimal B_m/B *vs.* ϕ. No dominant difference between the groups is found in these figures. Fig. 6(c) and Fig. 6(d) show relations of $\varepsilon_r(P_u)$ *vs.* H/B and of the optimal B_m/B *vs.* H/B, respectively. Still, the figures show less difference within different H/B. Such phenomenon might be caused by the measuring error during the field tests or laboratory experiments, or some soil properties or behaviors had not been taken into account.

The second series of trial and error tests is to apply fixed B_m/B value ranging from 0.6 to 1.0 with increment of 0.01 on all data set and evaluate their relative error of the uplift capacity to find the optimal B_m/B. In Fig. 7(a), the solid line shows the testing results of B_m/B with 37 sets of data and $B_m/B = 0.67$ has the best approach, the averaged $\varepsilon_r(P_u)$ is 0.2475 ± 0.0648 (see the last column in Table 3). Even though $B_m/B = 0.67$ is not better than the optimal B_m/B value, the approach is still better than previous theories and is easy for practical uses. Columns 14 to 16 in Table 2 show the results of the tests, including the optimal B_m/B, $P_{u,Net}$, and $\varepsilon_r(P_u)$. The results are

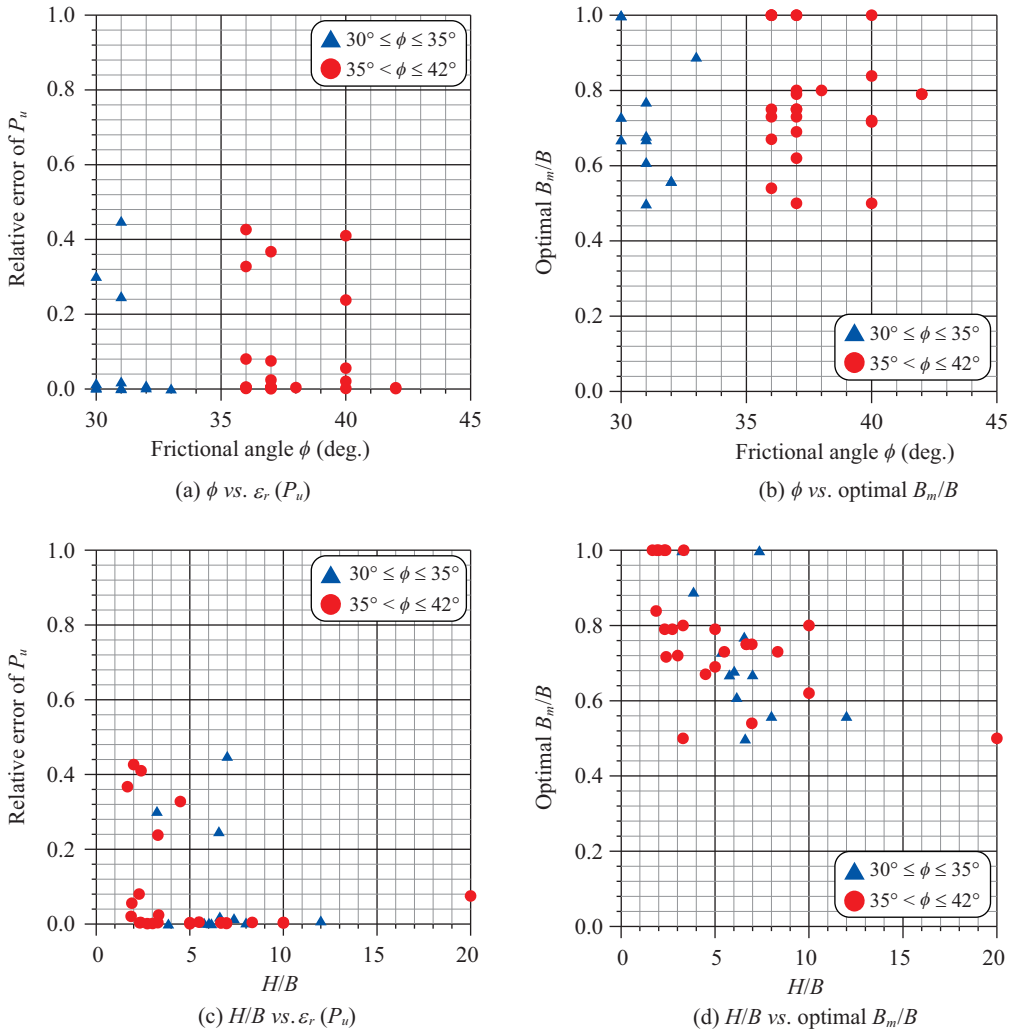

Fig. 6. Observations in optimal B_m/B tests.

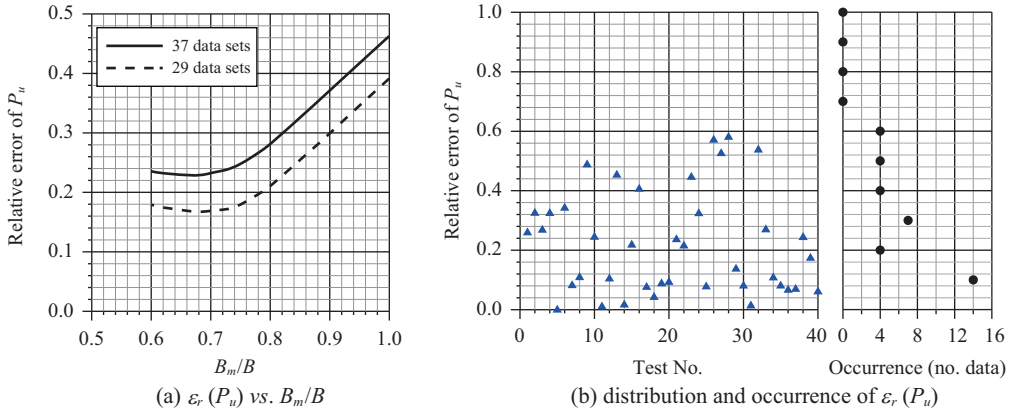

Fig. 7. Relative error $\varepsilon_r(P_u)$ analyses for $B_m/B = 0.67$.

also shown in Fig. 3 with symbol of ★. Fig. 7(b) plots the distributions of $\varepsilon_r(P_u)$ and the occurrence of $\varepsilon_r(P_u)$ for all data set. As shown in Table 2, there are 12 sets over-estimated and 25 sets under-estimated, but there also 19 sets have $\varepsilon_r(P_u)$ smaller than 0.2. If omitting the 8 data sets (No. 9, 10, 16, 23, 24, 26, 27, and 32 in Table 2, marked in light gray) for their relative errors are larger than 0.20 in optimal B_m tests, the averaged $\varepsilon_r(P_u)$ can be reduced to 0.1717 ± 0.0542 with the

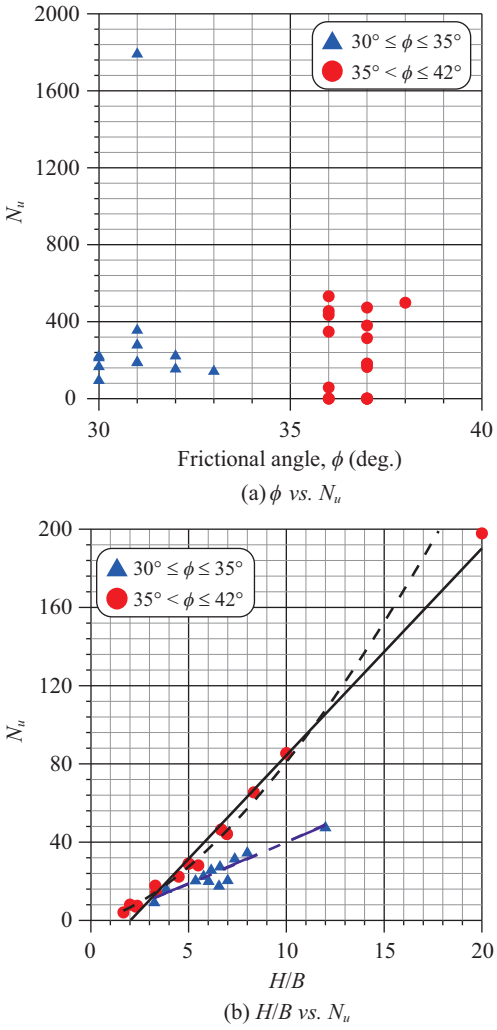

Fig. 8. Observations of N_u for $B_m/B = 0.67$.

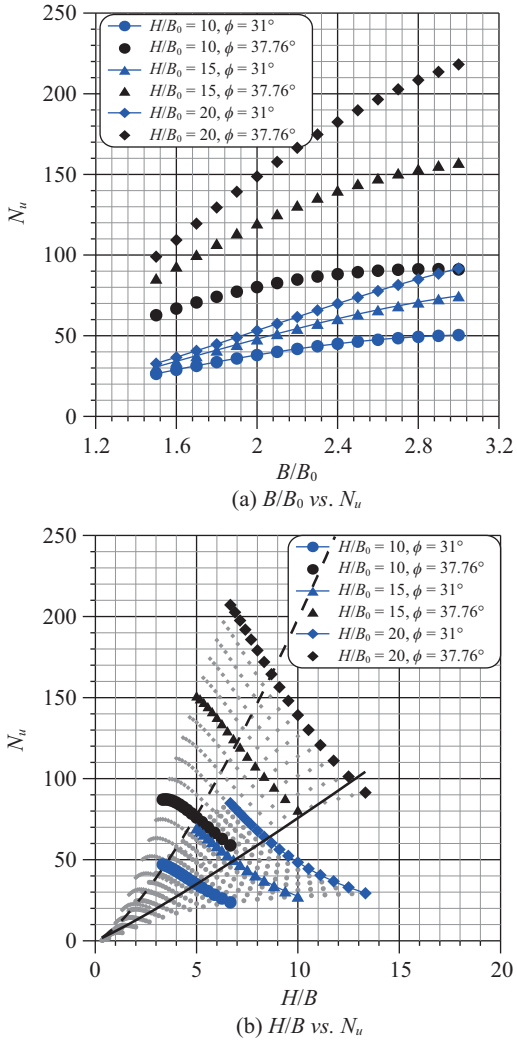

Fig. 9. Observations of B/B0 for $B_m/B = 0.67$.

same suggested B_m/B value. The relation between $\varepsilon_r(P_u)$ and B_m/B is plotted with dashed line in Fig. 7(b).

The third test is to investigate the relation between ultimate uplift capacity and the property of soil and pile with B_m/B = 0.67. Fig. 8 plots the relations of ϕ *vs*. N_u and H/B *vs*. N_u. The data are separated into two groups in accordance with the frictional angle of soil. In Fig. 8(a), no dominant relation was found between ϕ and N_u. In Fig. 8(b), linear (solid line) and power (dashed line) approximation curves are shown for each sand group. From the coefficient of determination and the residual mean square, the relation between N_u and H/B has better approximation by using the power expression for $H/B \le 10$. The loose sand has smaller ultimate uplift capacity than the dense sand. The approximate regression functions are shown as follows.

(1) Linear regressions

For loose sand ($30° \le \phi \le 35°$):

$$N_u = 4.2403(H/B) - 2.3737 \text{ (12 data sets)} \quad (23)$$

For dense sand ($35° < \phi \le 42°$):

$$N_u = 10.5748(H/B) - 21.4715 \text{ (25 data sets)} \quad (24)$$

(2) Power regressions

For loose sand ($30° \le \phi \le 35°$):

$$N_u = 1.1318(H/B)^{1.1104} \text{ (12 data sets)} \quad (25)$$

For dense sand ($35° < \phi \le 42°$):

$$N_u = 2.2068(H/B)^{1.5639} \text{ (25 data sets)} \quad (26)$$

Fig. 9 is the experimental results of the evaluations of the influences of different B/B_0 and H/B on N_u. The averaged density is set at 19.0, and B/B_0 is tested from 1.5 to 3.0 with $H/B_0 = 10$, 15 and 20 and $B_m/B = 0.67$. The frictional angle ϕ is set at 31° for loose sand and 37.76° for dense sand in accor-

dance with the mean frictional angle of the tested data. Fig. 9(a) shows that N_u will increase as H/B_0 getting larger, and N_u of dense sand is larger than that of loose sand; Fig. 9(b) shows the relations between H/B and N_u, the light gray symbols in the background are the numerical results from Eqs. (25) and (26) with different H/B_0 for reference. N_u was found increased as H/B_0 increased, but decreased as H/B increased of the same H/B_0. The tendency of the variations of N_u *vs.* H/B for all H/B_0 is the power curve relation shown as follows

For loose sand ($\phi = 31°$ and $\gamma_S = 19$):

$$N_u = 5.7614\left(H/B\right)^{1.1177} \tag{27}$$

For dense sand ($\phi = 37.76°$ and $\gamma_S = 19$):

$$N_u = 8.6843\left(H/B\right)^{1.3586} \tag{28}$$

V. CONCLUSIONS

(1) The enlarged base of the belled pile has positive influence on the uplift capacity of the pile. The uplift capacity is increased as the dimension of enlarged base increased.
(2) Due to the consolidation of the soil above the enlarged base caused by the uplift motion of the pile, the resultant failure surface develops from the surface of the enlarged base instead of from the tip of the vertical pile. According to the collected field/laboratory data, the starting location of the failure surface B_m is suggested equal to $0.67B$.
(3) The uplift capacity is affected by the frictional angle of the soil. The dense sand ($35° < \phi \leq 42°$) has larger uplift capacity than loose sand ($30° < \phi \leq 35°$).
(4) The uplift capacity N_u is increased as H/B_0 increased, but decreased as H/B increased of the same H/B_0.
(5) Due to the possible measurement error might occur during the field tests or laboratory tests, and incomplete soil properties collection, more data is needed to confirm the suitable starting location of the failure surface B_m.
(6) Part of the approximation error might be caused by treating the soil density to be uniform which neglect the consolidation of the soil above the enlarged base.

REFERENCES

Andreadis, A. and R. C. Harvey (1981). A design procedure for embedded anchors. Applied Ocean Research 3(4), 117-182.

Balla, A. (1961). The resistance to breaking out of mushroom foundations for pylons. Proceedings of the 5th International Conference on Soil Mechanics and Foundation Engineering, Paris, France, 1, 221-227.

Chattopadhyay, B. C. and P. J. Pise (1986). Uplift capacity of piles in sand. Journal of Geotechnical Engineering 112(9), 888-904.

Clemence, S. P. and C. J. Veesaert (1977). Dynamic pull out resistance of anchors in sand. Proceedings of International Symposium on Soil Structure Interaction, Roorkee, India, 389-397.

Dickin, E. A. (1988). Uplift behaviour of horizontal anchor plates in sand, Journal of Geotechnical Engineering. ASCE 114(11), 1300-1317.

Dickin, E. A. and C. F. Leung (1983). Centrifugal model tests on vertical anchor plates. Journal of Geotechnical Engineering, ASCE 109(12), 1503-1525.

Dickin, E. A. and C. F. Leung (1990). Performance of piles with enlarged bases subject to uplift forces. Canadian Geotechnical Journal 27, 546-556.

Downs, D. I. and R. Chieurzzi (1966). Transmission tower foundations. Journal of the Power Division, ASCE 92(P02), 91-114.

Frydman, S. and I. Shaham (1989). Pull out capacity of slab anchors in sand. Canadian Geotechnical Journal 26, 385-400.

Ghaly, A., A. Hanna and M. Hanna (1991). Uplift behavior of screw anchors in sand. I. Dry sand. Journal of Geotechnical Engineering, ASCE 117(5), 773-793.

Kulhawy, F. H. (1985). Drained uplift capacity of drilled shafts. Proceedings of 11th International Conference on Soil Mechanics and Foundation Engineering, San Francisco 3, 1549-1552.

Lin, C. H. (1998). A study on ultimate uplift capacity of belled piles in sand. Master thesis, Department of Harbor and River Engineering, National Taiwan Ocean University, 59 pages. (in Chinese)

Meyerhof, G. G. and J. I. Adams (1968). The ultimate uplift capacity of foundations. Canadian Geotechnical Journal 5(4), 225-244.

Murray, E. J. and J. D. Geddes (1987). Uplift of anchor plates in sand. Journal of Geotechnical Engineering, ASCE 113, 202-215.

Ovesen, N. K. (1981). Centrifuge tests to determine the uplift capacity of anchor slabs in sand. Proceedings of 10th International Conference on Soil Mechanics and Foundation Engineering, Stockholm, Sweden, 1, 717-722.

Rowe, R. K. and E. H. Davis (1982). Behaviour of anchor plates in sand. Geotechnique 32(1), 25-41.

Shanker , K., P. K. Basudhar, N. R. Patra (2007). Uplift capacity of single piles: predictions and performance. Journal of Geotechnical & Geological Engineering, Springer 25, 151-161.

Surtherland, H. B., T. W. Finlay and M. O. Fadl (1983). Uplift capacity of embedded anchors in sand. Proceedings of 3rd International Conference on the Behaviour of Offshore Structures, Cambridge, Maryland. 2, 451-463.

Tucker, K. D. (1987). Uplift behavior of drilled shaft and driven piles in granular soils. Foundations for Transmission Line Towers, ASCE Geotechnical Special Publication 8, New York, 142-159.

Verma, A. K. and R. K. Joshi (2010). Uplift load carrying capacity of piles in sand. Indian Geotechnical Conference-2010 (GEOtrendz), Mumbai, Maharashtra, India, 857-860.

Vermeer, P. A. and W. Sutjiadi (1985). The uplift resistance of shallow embedded anchors. Proc., of 11th Int. Conf. of Soil Mechanics and Foundation Engineering, 3, San Francisco, 1635-1638.

Vesic, A. S. (1971). Breakout resistance of objects embedded in ocean bottom. Journal of Soil Mechanics and Foundation, ASCE 97(9), 1183-1205.